Turkish Journal of Electrical Engineering & Computer Sciences

http://journals.tubitak.gov.tr/elektrik/

Research Article

Turk J Elec Eng & Comp Sci
(2015) 23: 1127 – 1141

doi:10.3906/elk-1212-166

A model-based edge estimation method with increased edge localization accuracy for medical images

Mehmet ÖZTÜRK*, Temel KAYIKÇIOĞLU
Department of Electrical and Electronics Engineering, Faculty of Engineering, Karadeniz Technical University, Trabzon, Turkey

Received: 28.12.2012 • **Accepted/Published Online:** 22.07.2013 • **Printed:** 10.06.2015

Abstract: This study proposes an improved method based on a nonlinear parametric model for intensity profile to increase the edge localization accuracy in medical images gathered from different imaging modalities. The edge model consists of three parameters associated with an edge point. It also takes into account local background intensity, noise, and blurring. The Marquardt–Levenberg algorithm is used to estimate the parameters because of its accuracy and good convergence rate. Performance of the proposed method is tested quantitatively by comparing the results with those of the well-known active contour method on synthetic vessel images. Qualitative comparisons on real MRI, coronary angiography, CT, ultrasound, and retinal images showed that the proposed method accurately estimates edges in medical images.

Key words: Edge estimation, medical image, parametric edge model, edge localization accuracy

1. Introduction

The importance and use of medical electronics are increasing gradually in parallel with the rapidly developing techniques of the technological age. Imaging techniques constitute the most important part of medical electronics, especially since they are being used in the diagnosis process. Medical imaging techniques have become more than just an imaging device or an instrument used to examine anatomic structures. They serve important roles, such as being planning appliances for a possible surgical intervention or radiotherapy; additionally, they are used to observe the progression of disease. However, some operations need to be conducted in order for these images to be evaluated. Edge detection methods are foremost among these techniques.

Edge information or contours related to the object of interest bear important information about that object in an image. The detection of edges is also a key step for further processing of images using techniques such as object recognition, segmentation, and 3D reconstruction. Therefore, edge detection on medical images captured with different imaging modalities has always been an open research field. Different imaging modalities result in images with different features. Therefore, developing a method that will reveal the best results for all kinds of medical images has always been a main motivation in this area of research.

Classical edge detection methods like derivative-based methods [1,2] are easy to apply. However, these techniques may fail to succeed due to factors such as high gray level alterations because of noise and discontinuity of edge areas originating from the nature of imaging modalities. These factors results in false detection of edges [3]. Different techniques were developed to overcome these problems. Some of these methods make a series of

*Correspondence: mehmetozturk@ktu.edu.tr

operations on the images with different resolutions in order to overcome effects such as noise and blurring in images [3–6]. These methods, which produce good results, require the regulation of some parameters based on trial and error. Other methods try to detect the edges either by modeling the morphological structure of the object or recognizing the tissues that belong to the object [7,8]. There are also methods that use a genetic algorithm or artificial intelligence [9]. These methods have a disadvantage of heavy calculations and memory use. In addition, there are region-based approaches based on the similarity feature of the objects in the images [10]. Clustering-based approaches are the most used methods among these [11,12]. However, in noisy images, these methods also fail to extract the correct edge information of the object of interest.

In this study, edge estimation is realized by using a parametric edge model developed to obtain the most accurate results with images that are collected from different imaging techniques. The model will be explained in more detail in the following sections. This model improved two points according to the previous studies [13,14]: the first improvement is the use of parametric active contours (snakes) instead of spline interpolation for the selection of initial profiles. The selection of initial profiles is crucial for the success of the method. Use of the active contour approach provides continuously changing initial profiles while keeping them sufficiently close to real edges. The second improvement is the use of the edge continuity property by applying constrained parameter estimation. These points will be explained in detail in the following sections.

This study is organized as follows: in Section 2, edge intensity profile modeling is explained, and then the selection of the region of interest is discussed. Parameter estimation is then explained for the profiles of the selected region. In Section 4, we discuss the differences of our method from previous methods and offer suggestions related to the alterations that can be made in future studies.

2. Proposed method

The proposed method is a semiautomatic edge estimation procedure. Figure 1 shows the main steps of the method. First we present some background information about the motivation of the method in the following subsection.

2.1. Modeling of edge intensity profile

In this study, we propose an edge estimation method based on parametric modeling. Parametric modeling methods give more accurate results than derivative-based methods because of modeling of the background and blurring effects on the medical images [13–16]. The fundamentals of the proposed method are based on the elliptical cross-section of a vessel model. Figure 2 shows a computer-generated vessel model. This vessel is modeled with a generalized cylinder with elliptical cross-sections.

In Figure 2, we also show incoming X-ray planes that intersect with the vessel model. These planes are calculated in such a way that their normal vectors coincide with the tangent vectors of the vessel center-line at the corresponding points. The intersection regions of the planes and vessel model will also be an ellipse because we use an elliptical cross-sectional generalized cylinder. These ellipses are defined in the local coordinate system that is characterized according to the local tangent vectors. Figure 3 shows an example of these ellipses and the corresponding computer-generated X-ray projection profile.

As a result of the experimental studies that we conducted with medical images that were obtained via methods such as MRI, CT, and angiography, we observed that the intensity profile of an object's edge can be modeled as the addition of object (the projection profile model) and background profiles. The mathematical

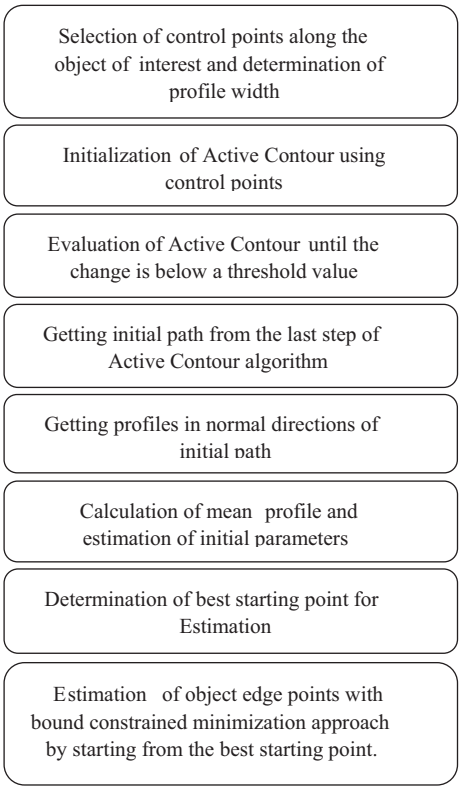

Figure 1. Flowchart of the proposed method.

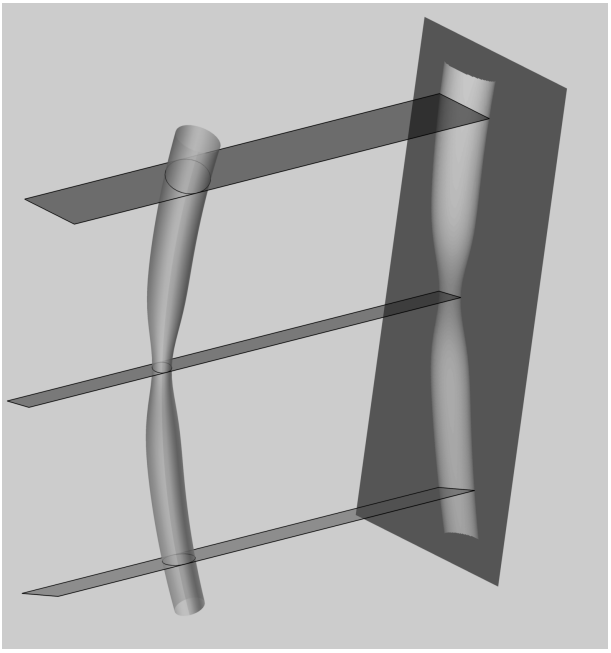

Figure 2. A computer generated vessel model and its projection on imaging plane.

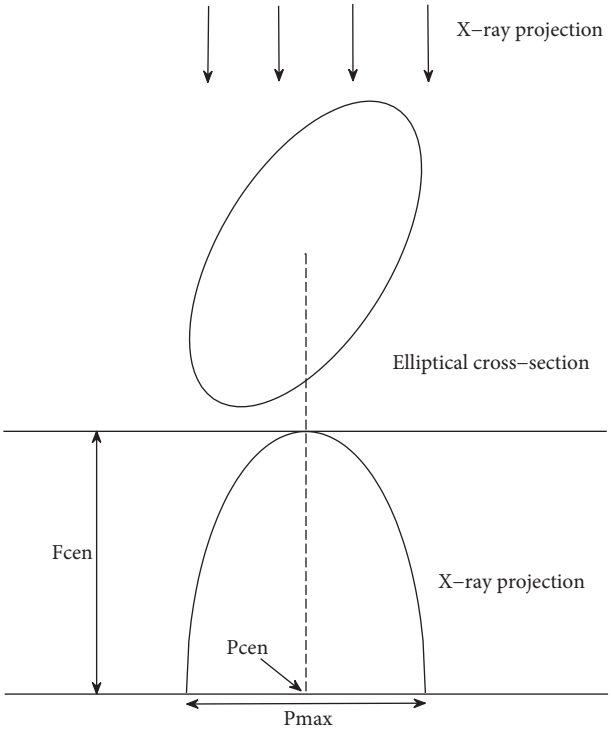

Figure 3. An elliptical vessel's cross-section and X-ray projection profile.

expression of the edge intensity profile of the object (the projection profile seen in Figure 3) is:

$$f(p) = (f_{cen}\sqrt{1-(\frac{p-p_{cen}}{p_{\max}})^2}\ ),\ p_{cen}\text{-}p_{\max} \leq\ \ p\ \ \leq p_{cen}+p_{\max}. \tag{1}$$

In this expression p, f_{cen}, p_{cen}, and $p_{\max}$ represent the horizontal axis (in pixels), the maximum value of the vessel lumen (in gray levels), the point that corresponds to the peak value (in pixels), and the cross-section width in the corresponding plane (in pixels), respectively. Consequently, p_{cen}, $p_{\max}$, and f_{cen} are parameters of an object's intensity profile. For tubular objects such as vessels, $p_{cen}-p_{\max}$ corresponds to the left edge coordinate while $p_{cen}+p_{\max}$ corresponds to right edge coordinate. As for objects other than vessels, a single edge point is valid since the right side of p_{cen} is ignored in terms of object intensity expression; therefore, its coordinate is determined via $p_{cen}-p_{\max}$ with subpixel accuracy. Similarly, the intensity expression of background $b(p)$ can be modeled with a fifth-order polynomial that ignores its second- and fourth-order terms to avoid wrong-fitting results at the center part of the model. The mathematical expression of the total profile was modeled as below, including noise and blurring effects as a result of nonlinear operations in the imaging process:

$$i(p) = f(p,\varphi) * g(p) + b(p) + w(p). \tag{2}$$

In this expression, * represents convolution, $g(p)$ represents a Gaussian-type blurring function that has an average of zero and a standard deviation of S, and $w(p)$ represents the Gaussian-type noise that has an average of zero and a standard deviation of σ.

Figure 3 shows the visual results of the experiments. In these experiments, we take sample profiles along an edge of an object of interest. The images used in this experiment are from ultrasound (Figure 4a), retinal angiography (Figure 4b), MRI (Figure 4c), CT (Figure 4d), and X-ray angiography (Figure 4e). We take the mean of all profiles to obtain a typical single profile for that image type. After that, we fit the proposed model to see how successfully we can represent these profiles.

The model fitting results can be seen in Figure 5. These tests show that our proposed model can successfully represent these profiles from different kinds of imaging modalities.

2.2. Detecting the region of interest (ROI)

We used a spline interpolation method as in previously proposed studies [13,14]. This method requires control points from the user to interpolate a path along the edge of an object of interest. The control points have to be set accurately and with a sufficient number to be able to initialize a useful path along the edge of the object of interest. The path selection method is replaced with a more versatile and robust method in this study. We used a parametric active contour model as a preprocess to obtain an initial guess of edge points. Therefore, the points defined by the user are used to initialize the active contour model.

In the literature, there are two types of active contours: parametric and geometric active contours. The main difference comes from the definition of curves (contours) that evolve in a digital image. This curve deforms under the effect of two types of forces, which are called internal and external forces. Both types of active contour models search for a state to balance their internal and external energy functions. Internal energy tries to keep the active contour smooth while external energy pulls the contour through the edges of the object of interest. The external force of active contours (either parametric or geometric) usually depends on the derivative of the image since we deal with edge features. Since the derivative-based edge estimation methods generate bias error due to blurring effect [17], this problem requires scale-space processing of the image, which needs large memory

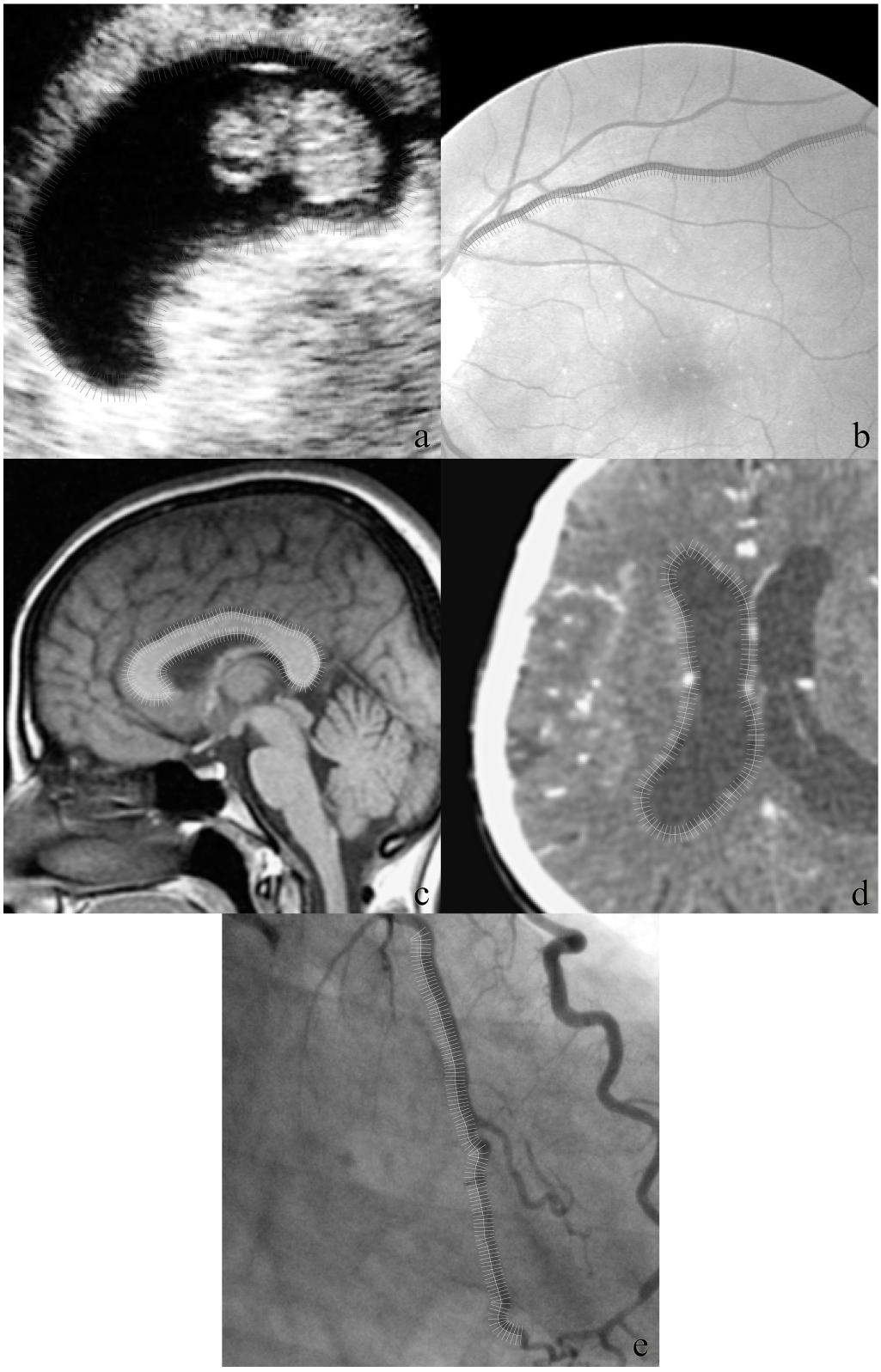

Figure 4. Selection of profiles from different imaging modalities: (a) ultrasound, (b) retinal angiography, (c) MRI, (d) CT, and (e) X-ray angiography.

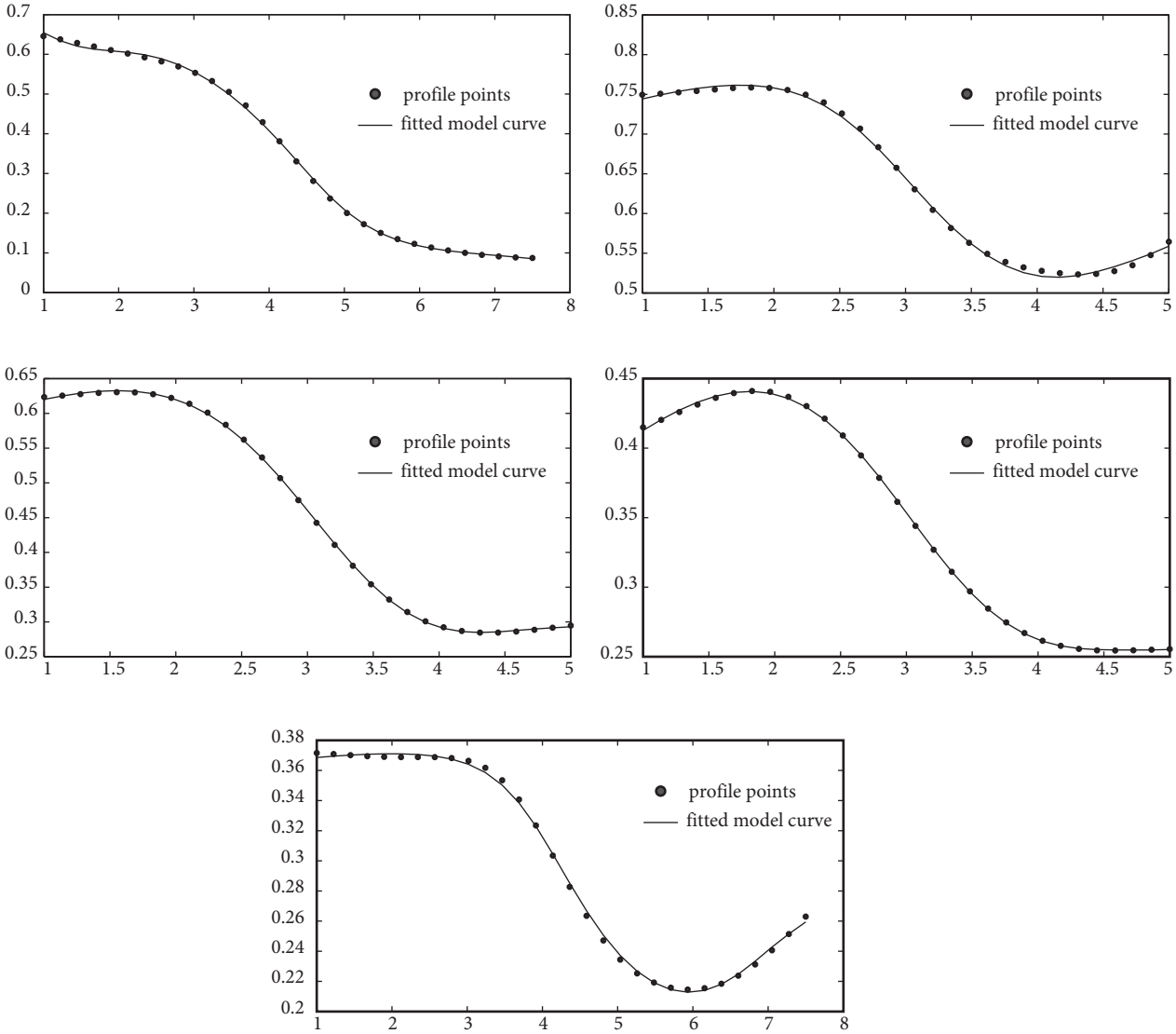

Figure 5. Edge profiles and their model fitting results. The dots correspond to profile points and the continuous curve is the fitted model.

and heavy calculations. Thus, usage of active contours by itself will not generate accurate edge estimations even if we set tighter convergence criteria and require longer computation times. We use active contours here instead of a spline interpolation-based technique to get a fast and rough estimate of initial profiles. Using active contours allows the user more flexibility for setting initial points and results in a more accurate initial path than the spline interpolation method. The initialization of the contour algorithm starts by linear interpolation of control points to obtain the parametric curve. This curve evolves under the influence of external and internal energy function until the change in the shape of the curve is less than a predefined threshold. The external energy used in this study is calculated from the derivative of the image with the vector flow convolution [18] approach for its good capture range. With properly determined weighting constants for internal and external energy functions (selected 1 for both of the constants throughout this work), the final shape of the contour (initial path) will be sufficiently smooth while it is close to the edges of the object. The smoothness of the initial edge line is crucial for the parameter estimation step in the modeling-based algorithm to use the continuity property of an edge.

The continuity property is used to get a robust edge detection method. Therefore, the active contour model provides a fast way to get continuously changing profiles along the edges of the objects.

After getting the initial edge path with the help of the active contour, the algorithm calculates normal vectors of every point on the path. These vectors are used as the profile selection directions within a properly selected range. This range is determined by the user according to the width of the object of interest. The intensity profiles are obtained by bilinear interpolation of the image at the profile selection points.

2.3. Estimation of model parameters

Since the projection model that we use is nonlinear, the Marquardt–Levenberg estimation algorithm, which is advantageous in terms of speed and a good convergence rate, was used to calculate parameters.

The Marquardt–Levenberg algorithm requires initial parameters for the estimation process (as well as other nonlinear minimization methods). The proximity of these parameters to the actual values both decreases the convergence rate of the algorithm and increases the percentage of attaining the most accurate result. In addition, the method must be robust against noise and abrupt changes caused by the background. For this purpose, we used the continuity property of the object parameters (f_{cen},p_{cen},p_{max}) by using the constrained minimization approach. Constrained minimization includes bounded change only in the object parameters with respect to the nearby profile parameters. We limit the change only to the object parameters because they must be continuous along its edge points. On the other hand, other parameters such as background profile parameters or the blurring parameter are not necessarily continuous.

The use of the continuity property requires a good initial guess to start with in the estimation process. It is possible to estimate the initial parameters from the profile with derivative-based approaches. This is useful for relatively flat background profiles or high contrast regions. On the other hand, for low contrast profiles or profiles that include other backgrounds, structure can cause the estimation to go wrong. Most of the time, the derivative-based methods fail to get a correct initial guess and this affects the convergence rate and success possibility of the nonlinear estimation. There is also a strong possibility of converging for the nonsuitable parameter vector. A global minimum will not necessarily give the correct values we expect because we are using the sum of two different models (a nonlinear vessel model and a linear polynomial background model) for estimation. We changed the method for estimating the initial parameters applied in the previous paper because of the need for robust initial parameter estimations [14]. For this purpose, we take the mean of the selected profiles and use this to estimate the initial parameters. The noise content and unwanted background effect will be decreased in this new profile because we took the mean. This helps to find the correct initial guess automatically by derivative operators. After determining the initial parameters, we searched for the profile that was most similar to the mean profile because we used the result of the previous estimation step as the initial guess for the next one. Therefore, we have to start with the profile that is the most similar to the mean profile. The similarity is measured by calculating the mean-squared error of the mean profile and the candidate. The minimum error profile is used to start the estimation process with the initial guess obtained from the mean profile.

There is the possibility of converging for an unwanted parameter vector because of the abruptly changing nature of the background, even if we start the minimization process from a good parameter vector. To reduce this possibility, we implied a bound restriction on the amount of change for the parameters of the next profile according to the previous one. This restriction is applied only for the object parameters because the background is not necessarily continuous. Therefore, we searched for the correct object parameters within the region that are determined by the previous parameter vector. In fact, with the limitation of parameter change, we define

a maximum and minimum for the next profile parameters. Therefore, the width of the search region for every parameter depends on the sampling interval of the ROI and closeness of the initial profiles to the actual edges. Initial profiles are determined with active contours. Since this method is also a robust edge estimation approach, we make an accurate estimate for every profile. The performance of the improvements against the previous approach is demonstrated with tests; it is presented in the next section.

3. Experimental results

First we compared the proposed method with the one presented previously [14] to show how well the proposed improvements operate. For this purpose, we produced a synthetic vessel image and added a real angiography image as background. The artificial vessel has a constant radius along its centerline. The vessel parameters are: f_{cen}: *10,20,30,40,50* (gray levels);p_{cen}: *256* (pixels);p_{max}: *5* (pixels); and blurring level *(sigma)*: *1.35* (pixels). The constants for the polynomials (background model) are selected as zero due to the addition of the real angiography image as a background. The noise is also is not added to the profiles for the same reason. The aim here is to show the effect of constrained optimization on the edge estimation process. The initialization of the path along the vessel was realized with a constant line along the real edge with a 2-pixel bias error. This bias is intentionally added to emphasize the performance of the estimation process against initialization errors. Since we take the profile interval as 1 pixel, we chose the bound restriction limits as 1 gray level for f_{cen}, 0.2 pixels for p_{cen}, and 0.4 pixels for p_{max}. These restrictions imply that, for example, the $p_{max}(i)$ parameter will be searched within the region of p_{max} *(i-1)* $\pm$ *0.4*. The p_{cen} parameter is the center of the object so it is expected that p_{cen} will not change much according to the p_{max}. That is the reason for the selection of limits in that way.

We compared two algorithms for different contrast levels (f_{cen}). The results are presented over a distance error that is calculated between real and estimated edge coordinates. Table 1 shows the results for this comparison. Table 1 also shows that constrained estimation gives more robust estimation results than the previous method, especially for low contrast images.

Table 1. Comparison of the improved method with previous method in terms of estimation accuracy.

Contrast amount f_{cen} (gray levels)	Previous method (without constrained optimization), estimation error (pixels)		Proposed method (with constrained optimization), estimation error (pixels)	
	Mean	Standard deviation	Mean	Standard deviation
10	3.6233	1.9658	0.8122	0.7170
20	0.6705	0.6813	0.4147	0.3428
30	0.3104	0.2921	0.2964	0.2661
40	0.2436	0.2417	0.2282	0.2173
50	0.1964	0.1922	0.1915	0.1871

To present the tolerance of the model-based edge detection method, we tested our algorithm with ground truth edge parameters on the same synthetic image used in the previous experiment. The initial path is obtained from real edge points. This situation gives us the correct value of $p_{cen} - p_{\max}$ but not more. Thus, the algorithm has to estimate the correct values of all the parameters. This test shows us the edge localization accuracy under the conditions of ground truth initial path. Table 2 presents the results of this test for 5 different gray level values. The edge localization accuracy is presented over the mean and standard deviation of distance errors. If

we compare the results of Table 1 and Table 2 for the outcomes of the proposed method, it is easily seen that the results are almost identical. However, the initial path in the first experiment was added a 2-pixel bias error. We can therefore conclude that our proposed method is robust under initialization errors.

Table 2. Tolerance of the proposed method with different gray levels.

f_{cen}(in gray levels)	Localization error (in pixels) ($p_{\max}$ =*5 pixels*)	
	Mean	Standard deviation
10	0.7908	0.7415
20	0.3923	0.3498
30	0.2807	0.2649
40	0.2234	0.2200
50	0.1853	0.1913

We also made some visual comparisons to see the effect of constrained minimization. Figure 6 shows four different synthetic vessel image parts. These images are produced intentionally to fault the normal minimization approach with some background effects. In Figure 6, the left column shows estimations from the normal minimization approach (previous method), while the right columns are the results of the constrained minimization method. We can see from Figure 6 that the constrained minimization approach is a much more robust edge estimation approach against abruptly changing background effects.

We also have compared our method with the traditional active contour algorithm (snake method) on both computer-generated images and real images. We selected the active contour method because it needs a ROI, as with our proposed method. The quantitative results from artificially generated images show a major increase in the estimation of correct locations of edges with the proposed method. The qualitative results for real images also show the effectiveness of the proposed algorithm for the aspects of accuracy and robustness.

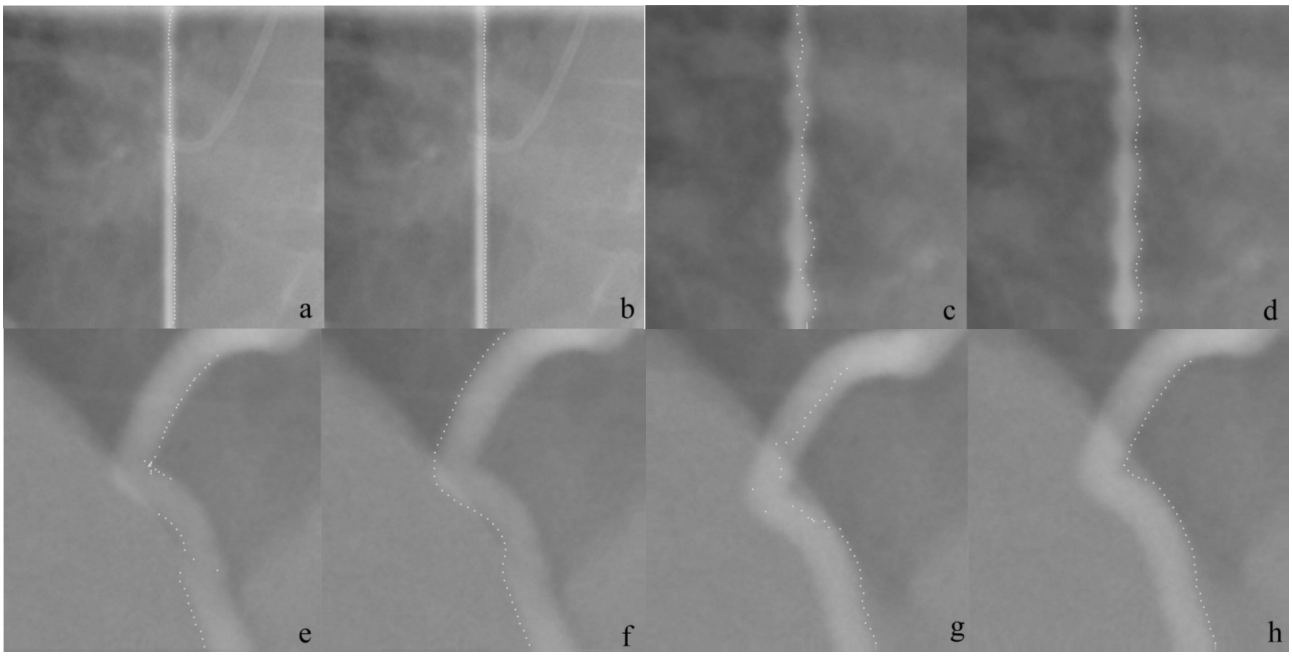

Figure 6. Visual comparison of the previous method with the proposed method. The left column shows estimations from previous method and the right column is from the proposed method. The robustness of the proposed method reveals itself in the tracking performance.

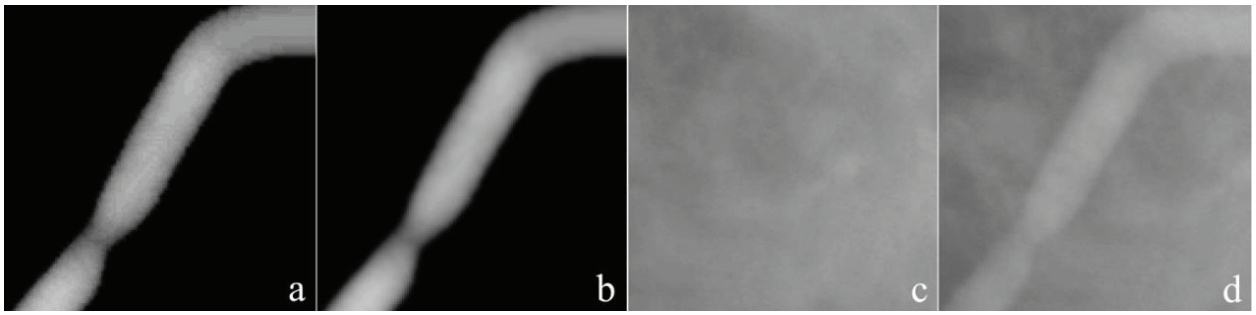

Figure 7. Synthetic angiogram image: projection of 3D vessel model (a), blurred vessel model (b), real background (c), and sum of blurred vessel model with the background (d).

Table 3. Hausdorff distance table.

	Sample 1	Sample 2
Between estimated edge points by active contour method and original edge points	1.1486	1.5623
Between estimated edge points by proposed method and original edge points	0.4817	0.5552

We produced a computer-generated vessel projection image to obtain a quantitative accuracy measure. First, a 3D generalized cylinder vessel model was produced. By simulating the angiographic imaging process with a ray tracing approach, we take a projection of this model on a 2D plane to get a simulated medical image without any background (Figure 7a). This image has provided us a vessel projection with known true edge locations. To produce a more real-like image we convolved the vessel projection with a Gaussian kernel to simulate the blurring effect (Figure 7b). After this step, we added a real angiogram image without any vessel projection (taken just before contrast increasing matter was injected) as the background (Figure 7c). The artificial image used in this experiment can be seen in Figure 7d.

To get a quantitative result, we calculated the Hausdorff distance [19] of the active contour method and our proposed method for the reference of the ground truth edge curve. The Hausdorff distance metric gives us a number that measures the similarity between two sets of points. A value of zero means these two sets are identical. For a verbal definition, the Hausdorff distance is the greatest of all distances of points from one set to the closest point from another set. Table 3 shows the results of this metric for two sample regions taken from the artificially generated image. We can see that the proposed method gives closer edge points than the active contour method.

Figure 8 shows the visual results of the accuracy comparison tests. The left column shows the original images used for the test and the right column shows comparisons. The dotted curve indicates the original edge of the vessel while the white one represents the estimated edge curve from the proposed method. The black curve is the result of the active contour method. This clearly demonstrates a significant bias error between the original and estimated curves by active contour method due to the blurring effect.

In the right column of Figure 8, we can see the performance of the proposed method by inspecting the closeness of the estimated curve to the original. We intentionally keep the contrast of the vessel low to show the performance better against the derivative-based active contour method. The proposed modeling approach outperforms the active contour method for the aspect of closeness to the real edge curve.

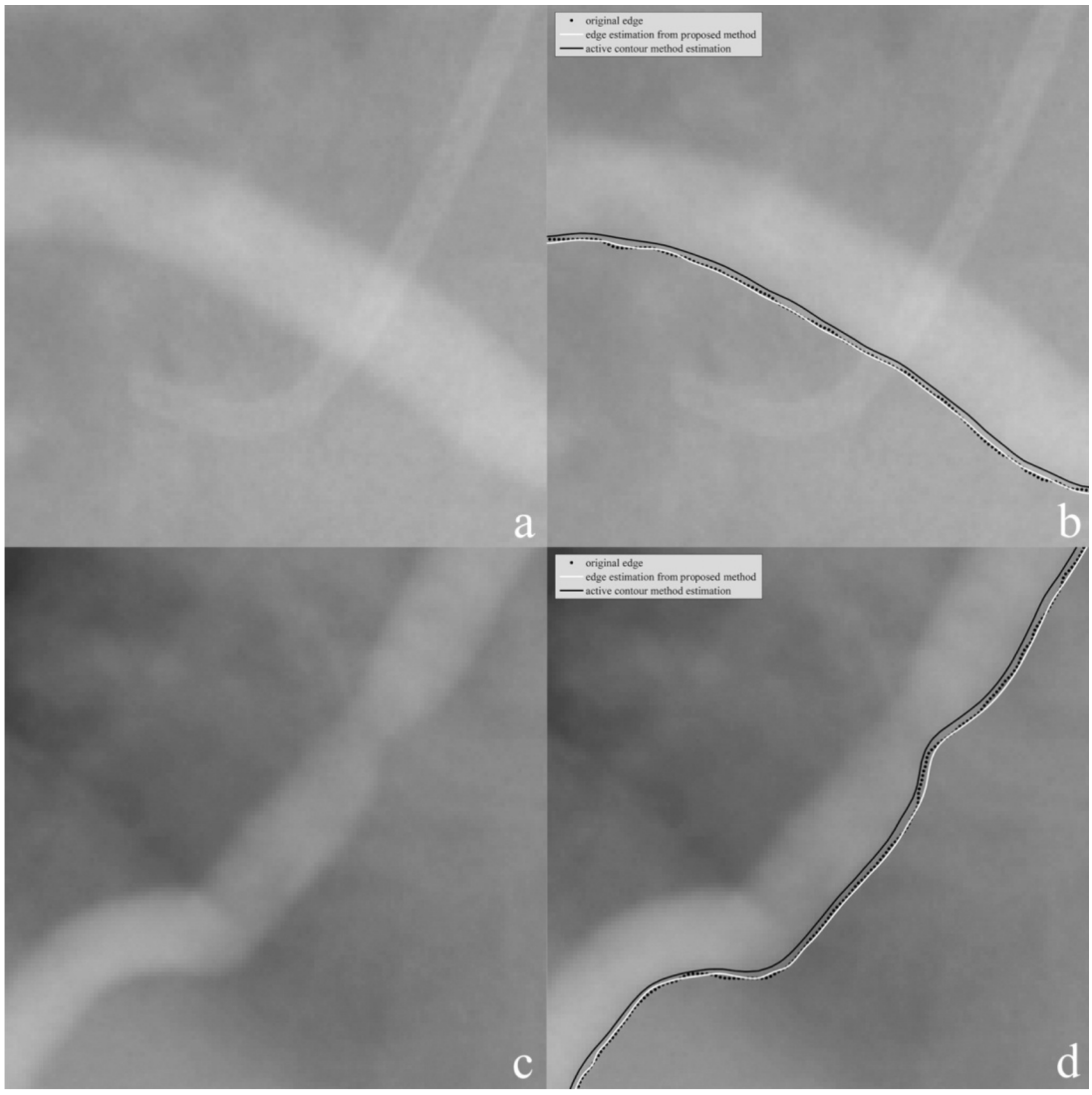

Figure 8. Visual comparison of the active contour method with the proposed method: original images (a, c) and estimated edges with the original edge curve (b, d).

Figure 9 shows two bifurcated vessel images from a real angiogram image. The white line indicates the estimation result of the proposed algorithm while the black line indicates active contour initialization path. These images (Figures 9a and 9b) are prepared to present the performance of the proposed method at two points. The first point is the effectiveness of the one-sided model at the bifurcated parts of the vessels. Our previously proposed method [13,14] uses the full profile of the vessel to estimate the two edge points of the vessel at the same time. This is useful for nonbranching tubular structures. However, if we try to model the bifurcation regions, we cannot use full profiles for estimation. Instead, one side of the vessel model will maintain the validity at the bifurcation points. The second point that we try to indicate with Figures 9a and 9b is the tolerance of the proposed algorithm to initialization errors. If we carefully examine the lower right part of Figure 9a and lower left part of Figure 9b, it is easily seen that the active contour initialized path missed the thinner parts of the vessel. This is a general problem of the active contour methods and requires regularization of some parameters in the active contour algorithm. However, our proposed method tolerates this type of error.

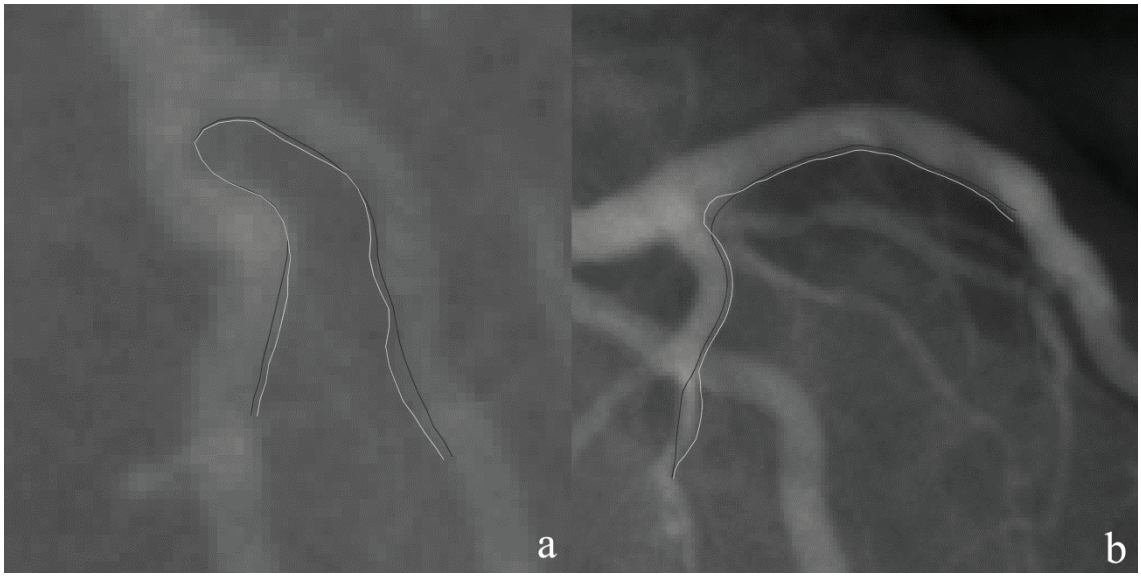

Figure 9. Performance test of proposed method on bifurcation points. White line is the estimation of the proposed method. Black line is the output of the initial active contour path.

We also qualitatively compare our model-based edge detection method with the active contour method on different kinds of real images taken from different devices. Although the motivation of the model-based edge detection method is based on the modeling of X-ray projections of vessels, we can easily model the edge profiles of other kinds of images. The following visual results showed that our method can be used for different kinds of images for edge detection purposes. In all the visual test results, the white dots stand for the proposed method estimations while the black ones represent the active contour method.

The first visual comparison test image was gathered from an angiogram device. Figure 10a shows an angiogram image. In all test images, the white dots indicate edge estimations by the proposed method and the black ones represent the active contour method. The active contour method uses gradient information of the image as an external force and hence showed some underestimation effect due to blurring. However, our modeling approach accurately estimated the correct locations of edge points by modeling both background and blurring. In Figure 10b, a retinal angiogram image is used to test the proposed method. Our method shows good performance, especially at the junction region of the traced vessel, because of modeling the background.

Other visual tests were conducted on MRI, CT, and ultrasound images. Figures 10c, 10d, and 10e show an MRI image, a CT image, and an ultrasound image, respectively. The proposed method outperforms the active contour method at the point of accuracy for all these images.

4. Discussion

This study used the application of an edge detection algorithm, which was previously proposed in [14], on medical images that were obtained by different techniques. The previous method is enhanced by the involvement of the active contour models and the continuity property of an edge. The active contour model is used for the selection of initial profiles in a smoothly changing manner while getting the initial edge points close enough to the real object edge. This provides the user more flexibility for the initialization process. On the other hand, smoothly changing profiles allow us to use the continuity feature of edge points at the estimation step. The second improvement is the use of the constrained optimization technique to get a robust edge detection method against noise or abrupt changes of background. We applied a limited change only on the object parameters

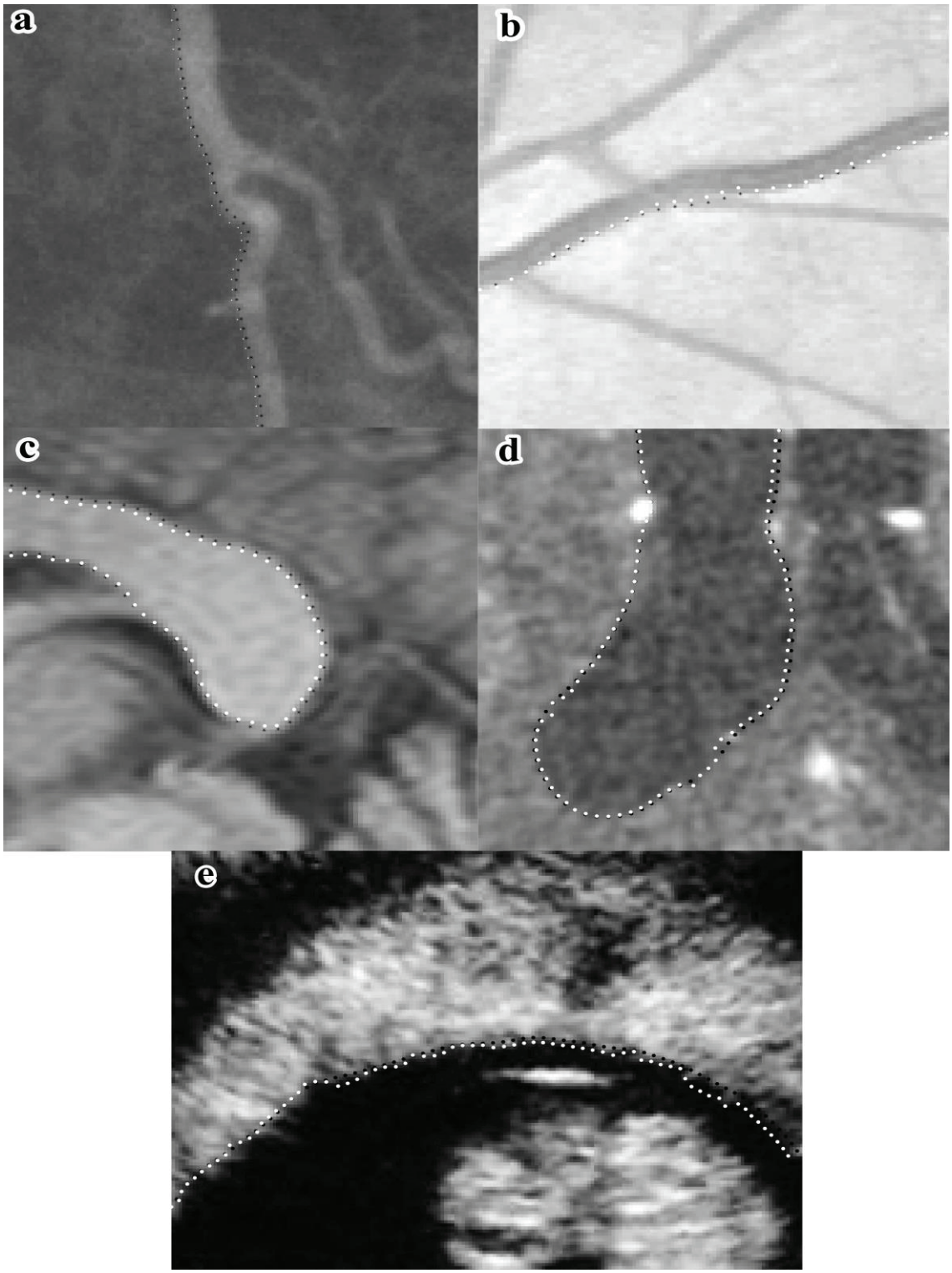

Figure 10. Visual comparison of the proposed method with active contour method on an angiogram image (a), a retinal angiogram image (b), an MRI image (c), a CT image (d), and an ultrasound image (e).

according to the previous parameters. By changing the constrained limits, we can control the smoothness of the estimated points.

Application of the model-based edge detection method to medical images provides more accurate edge estimations, as can be seen in the quantitative results. Especially with vessel images, accuracy is important for the diagnosis of illness, planning a treatment process, or tracking the progress of a disease. Therefore, our proposed method will be a robust and accurate edge detection tool for physicians.

There is no a reliable fully automatic edge detection method in the literature; therefore, semiautomatic methods with minimal interaction are more useful for users. Our method needs only a rough estimate for the edge region of the object of interest and a profile width in pixels. On the other hand, profile width has a very important effect on the accuracy and convergence of the method. The width of profiles must be selected in such a way that enough information for estimation could be gathered from them. As a future enhancement, the profile width selection will be determined automatically by application of multiscale operations.

References

[1] J. Canny, "A computational approach to edge detection" IEEE Transactions on Pattern Analysis and Machine Intelligence, Vol. 8, pp. 679–714, 1986.

[2] V. Chickanosky, G. Mirchandani, "Wreath products for edge detection", Proceedings of the IEEE International Conference on Acoustics, Speech and Signal Processing, Vol. 5, pp. 2953–2956, 1998.

[3] M. Shih, D. Tseng, "A wavelet-based multiresolution edge detection and tracking", Image and Vision Computing, Vol. 23, pp. 441–451, 2005.

[4] C. Bauer, H. Bischof "A novel approach for detection of tubular objects and its application to medical image analysis", Lecture Notes in Computer Science, Vol. 5096, pp. 163–172, 2008.

[5] Y. Zeng, C. Tu, X. Zhang, "Fuzzy-set based fast edge detection of medical image", Fifth International Conference on Fuzzy Systems and Knowledge Discovery, Vol.3, pp. 42–46, 2008.

[6] D. Qi, F. Guo, L. Yu, "Medical image edge detection based on omnidirectional multi-scale structure element of mathematical morphology", IEEE International Conference on Automation and Logistics, pp. 2281–2286, 2007.

[7] V.S. Thangam, K.S. Deepak, G.N.H. Rai, M.P. Prabhakar, "An effective edge detection methodology for medical images based on texture discrimination", Seventh International Conference on Advances in Pattern Recognition, pp. 227–231,2009.

[8] Z. Yu-Qian, G. Wei-Hua, C. Zhen-Cheng, T. Jing-Tian, L. Ling-Yun, "Medical images edge detection based on mathematical morphology", 27th Annual International Conference of the Engineering in Medicine and Biology Society, pp. 6492–6495, 2006.

[9] M. Gudmundsson, E.A. El-Kwae, M.R. Kabuka, "Edge detection in medical images using a genetic algorithm", IEEE Transactions on Medical Imaging, Vol. 17, pp. 469–474, 1998.

[10] R. Jain, R. Kasturi, B.G. Schunck, Machine Vision, New York, McGraw-Hill, 1995.

[11] C. Lai, C. Chang, "A hierarchical evolutionary algorithm for automatic medical image segmentation," Expert Systems with Applications, Vol. 36, pp. 248–259, 2009.

[12] Z. Beevi, M. Sathik, "A robust segmentation approach for noisy medical images using fuzzy clustering with spatial probability", International Arab Journal of Information Technology, Vol. 9, pp. 74–83, 2012.

[13] T. Kayikcioglu, S. Mitra, "A new method for estimating dimensions and 3-D reconstruction of coronary arterial trees from biplane angiograms", Sixth Annual IEEE Symposium on Computer-Based Medical Systems, pp. 153–158, 1993.

[14] H. Ture, T. Kayikçioglu, A. Gangal, "Doğrusal olmayan model kullanarak tıbbi görüntülerde kenar belirleme", Signal Processing, Communication and Applications Conference,2003 (in Turkish).

[15] T. Kayikçioglu, A. Gangal, M. Turhal, C. Kose, "A surface based method for detection of coronary vessel boundaries in poor quality x-ray images", Pattern Recognition Letters, Vol. 23, pp. 783–802, 2002.

[16] T.N. Pappas, J.S. Lim, "A new method for estimation of coronary artery dimensions in angiograms", IEEE Transactions on Acoustics, Speech and Signal Processing, Vol. 36, pp. 1501–1513, 1988.

[17] C.J. Kooijman, J.H.C. Reiber, J.J. Gerbrands, J.C.H. Schuurbiers, C.J. Slager, A.D. Boer, P.W. Serruys, "Computer-aided quantitation of the severity of coronary obstructions from single view cineangiograms", First IEEE Computer Society International Symposium on Medical Imaging and Image Interpretation, pp. 59–64, 1982.

[18] B. Li, S.T. Acton, "Active contour external force using vector field convolution for image segmentation", IEEE Transactions on Image Processing, Vol. 16, pp. 2096–2106, 2007.

[19] F. Hausdorff, Grundzüge der Mengenlehre, Leipzig, Veit, 1914 (in German).